# Deep learning transcriptomic model for prediction of pan-drug chemotherapeutic sensitivity

Eddie Guo[1], Mehul Gupta[2], Pouria Torabi[1], and Sunand Kannappan[2]

[1]University of Alberta
[2]University of Calgary

June 24, 2020

### Abstract

Emerging precision oncology studies have yet to generate a predictive biomarker that utilizes gene expression profiles to stratify tumours into similar pan-drug sensitivity profiles. This development would allow for identification of candidate drugs for treatments that maximize therapeutic response and minimize cytotoxic burden. As such, this study utilized cell line sensitivity and molecular profiling data to generate a combinatorial gene expression predictive biomarker, utilizing feature selection and a deep learning model. A cohort of cell line gene expression data from Genomics of Drug Sensitivity in Cancer (GDSC) was clustered into two response groups. Cell line response groups showed a significant difference in pan-drug chemotherapeutic sensitivity. Due to the high dimensional nature of the microarray data, biologically agnostic feature selection was conducted to identify genes with the highest predictive value. The feature space was reduced to 300 genes; functional profiling was enriched primarily for the focal adhesion, ECM-receptor and proteoglycan interaction pathways. Using these selected genes, a deep learning neural network architecture was developed to predict response groups. It was determined that a 4 hidden layer deep learning architecture was optimal for the dataset; following hyperparameter tuning, the model showed a predictive accuracy of 91.7% and precision of 94.4% (AUC = 0.872 ± 0.054). This validates the postulate that cell lines with similar gene expression profiles present similar pan-drug chemotherapeutic sensitivity, and it suggests the potential utility of similar combinatorial biomarkers for selection of potent candidate drugs.

### Keywords

clustering, neural network, transcriptomics, chemotherapeutic response, combinatorial biomarker, molecular profile, therapeutic sensitivity, cancer

## 1 Introduction

With the advent of high-throughput sequencing technology, precision oncology approaches have utilized molecular characteristics of tumours to inform clinical decision-making, including choice of chemotherapeutic regimen. The major focus of these approaches has been the development of targeted therapeutics, which are selective for specific genetic aberrations and expression profiles. Although these approaches may be successful for inducing tumour response, tumours are more likely to gain resistance to therapies with specific targets [1]. Moreover, not all tumours present with targetable features [1].

Emerging precision oncology approaches have begun to utilize high-throughput technology to potentiate the usage of conventional and less-targeted chemotherapy. Given that many of these less-targeted and consequently more cytotoxic chemotherapies have broad activity, the primary determinants of chemotherapeutic selection include cancer type and certain molecular markers [2]. Nevertheless, it is well established that tumour sensitivity to chemotherapy is heterogeneous both between and within cancer types, which results in a subset of patients that fail to respond to conventional chemotherapy regimens while being subjected to significant side effect burden [3]. Given that evidence suggests that gene expression can mediate drug response, recent advances have utilized individual and combinatorial gene expression biomarkers to develop predictors of tumour sensitivity to chemotherapeutic compounds [4].

While previous studies have developed predictive biomarkers for specific drugs, the utility of these biomarkers is limited to particular patients and clinical contexts [5]. That is, these studies are

limited in terms of clinical generalizability to different chemotherapeutic regimens. However, a pan-drug predictive biomarker may provide significant clinical utility in the selection of candidate therapies for particular patients. Such a biomarker could be developed if tumours with similar expression have similar drug responses across all chemotherapies, with few exceptions. The availability of pan-cancer cell line databases with *in vitro* drug sensitivity analyses along with accompanying gene expression profiling provides an ideal model for such analyses [6]. However, most previous drug sensitivity predictive biomarkers built on cell line databases have utilized classical machine learning combinatorial techniques, which fail to capture the dimensionality of available transcriptomic data. Furthermore, advanced deep learning algorithmic approaches that are capable of handling such dimensionality often fail to allow interpretability, and consequently require transcriptomic data that is clinically infeasible [7]. Thus, deep learning approaches should minimize the number of transcriptomic features selected to maximize both the accuracy and functionality of such predictive biomarkers.

As such, we set out to generate a deep learning transcriptomic model for the prediction of pan-drug chemotherapeutic sensitivity across cell lines of all cancer types. If successful, this would demonstrate that gene expression influences chemotherapeutic response across most drugs and further motivate future studies into the development of clinically applicable predictors of candidate chemotherapeutics for tumours of a specific gene expression profile.

Following unsupervised clustering of cell lines into therapeutic response groups with similar pan-drug sensitivity, we show that conventional clinical criteria fail to stratify cell lines by therapeutic response. We utilize a biologically agnostic feature selection algorithm to iteratively select and identify a subset of 300 relevant genes predictive of chemotherapeutic sensitivity. We then generate a combinatorial model from the selected genes utilizing neural networks that showcases a strong predictive ability across pan-cancer cell lines.

# 2 Methods

Here we developed a deep learning model to accurately classify cancer cell lines into therapeutic response groups using data from the Genomics of Drug Sensitivity in Cancer (GDSC) consortium. Following data collection and curation, we utilized unsupervised clustering algorithms to define two groups based on chemotherapeutic response. Next, we employed a biologically agnostic feature selection algorithm, Boruta, to select statistically relevant genes for our neural network. We developed an optimized neural network that utilizes transcriptomics features to classify patients into therapeutic response groups. See Fig. 1 for an overview of the data analysis pipeline.

## 2.1 Determining pan-cancer therapeutic response cohorts

To better understand the impact and predictive ability of transcriptomic dysregulation in chemotherapeutic response, a pan-cancer cohort of cell line and associated therapeutic sensitivity data were obtained from the GDSC database. This database includes 1,110 cell lines from various tumour types, and is thought to represent a relatively comprehensive pan-cancer set. In addition, the acquired dataset contained therapeutic efficacy information in the form of half-maximal inhibitory concentration ($IC_{50}$) values for 251 chemotherapies. These values correspond to the minimal concentration of therapeutic required to induce cell death in 50% of the cultured cells, with lower values being associated with improved drug efficacy. The data was used to generate a matrix with cell line and accompanying therapeutic information. This dataset was filtered to exclude therapies with less than 80% of data for all cell lines, followed by the exclusion of cell lines lacking response data for the drugs retained in the first step.

## 2.2 Identification of pan-cancer therapeutic response cohorts

Cell line therapeutic sensitivity matrices were used to evaluate whether conventional clinical criteria could separate patients into previously-defined chemotherapeutic response groups. These conventional clinical criteria included anatomic location and solid versus non-solid tumour status, as well as broadly applicable molecular markers – TP53 and KRAS mutation status [8, 9, 10, 11]. Cell lines were separated into subgroups based on these criteria and plotted to determine whether these criteria effectively clustered response groups.

Following evaluation of existing classifiers, we attempted to create defined cell line clusters on the basis of the observed chemotherapeutic response of the pan-cancer cell line sample. We developed a Euclidean distance matrix for the retained cell lines based upon their pan-chemotherapy response. This matrix was then used to identify the minimum number of clusters capable of representing the therapeutic heterogeneity identified across the cancer cell lines while maintaining significant inter-cluster distance. K-means clustering was then utilized to assign cell line candidates to appropriate therapeutic response cohorts. Generalized differences in chemotherapeutic efficacy between cohorts were visualized using a heatmap generated by the Pheatmap package in R. Separation between clusters was also visualized using principal component analysis with the factoextra package in R. Following the identification of defined clusters, differences in therapeutic efficacy between the identified cohorts
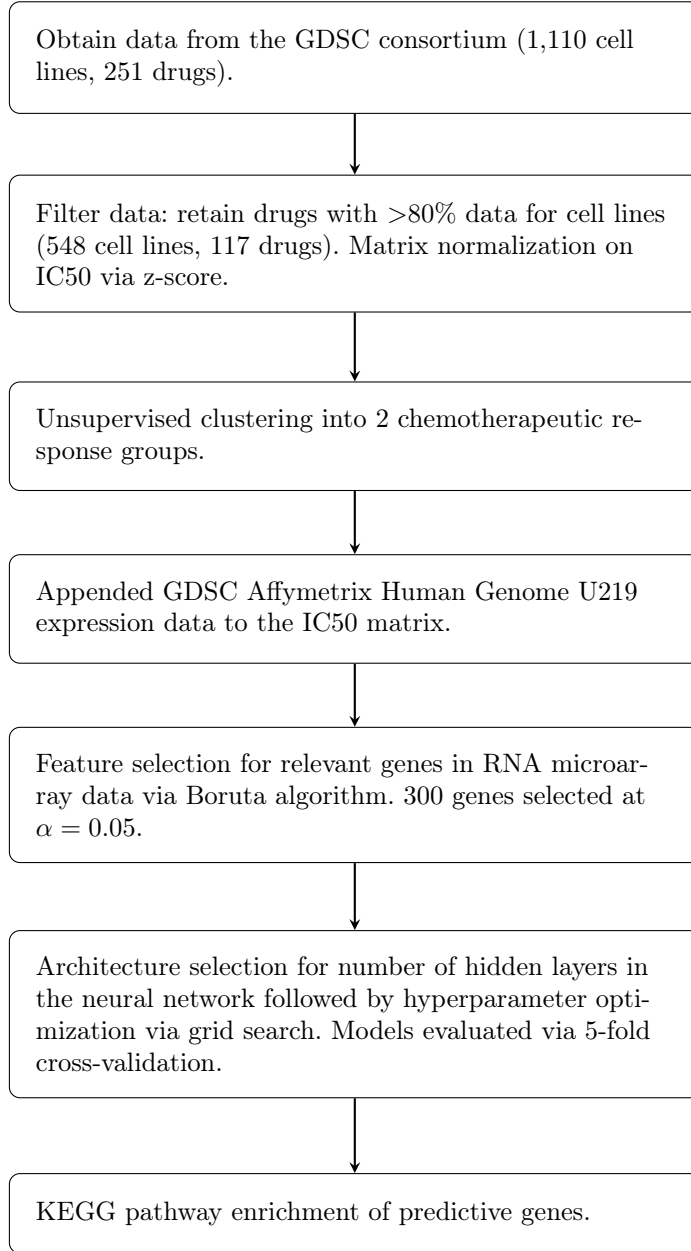
Figure 1: Summary of the data analysis pipeline.

were evaluated. Mann-Whitney U tests were utilized to compare $IC_{50}$ values between the groups. False discovery rate (FDR) correction was utilized to correct for multiple comparisons.

## 2.3 Feature Selection with Boruta

In order to develop a transcriptomic model predictive of therapeutic response clusters, we retrieved expression data quantified by the GDSC consortium using the Affymetrix U219 microarray for each candidate cell line. Here, minimally processed CEL files were obtained from ArrayExpress (ascension number E-MTAB-3610) and processed using the affy package in R. The resulting normalized expression matrix for candidate cell lines was then merged with the existing dataset. This addition resulted in the loss of 7 cell lines (2 from cluster A and 5 from cluster B), resulting in the inclusion of 541 cell lines in model generation. The microarray dataset quantified the expression of 16,382 genes; a model based on that many features is likely to overfit, compromising the generalizability of the model on new data. Such a large feature space also adds unnecessary noise and severely limits the accuracy and computational efficiency of the model. We addressed these issues feature selection via the BorutaPy package in Python 3 [12]. The BorutaPy package is a feature selection algorithm based on Random Forest classification which iteratively removes features that are statistically less significant than a shuffled version of the same feature [13]. Computational efficiency and the resulting feature set quality were motivators for choosing Boruta over other selection algorithms such as univariate selection or recursive feature elimination.
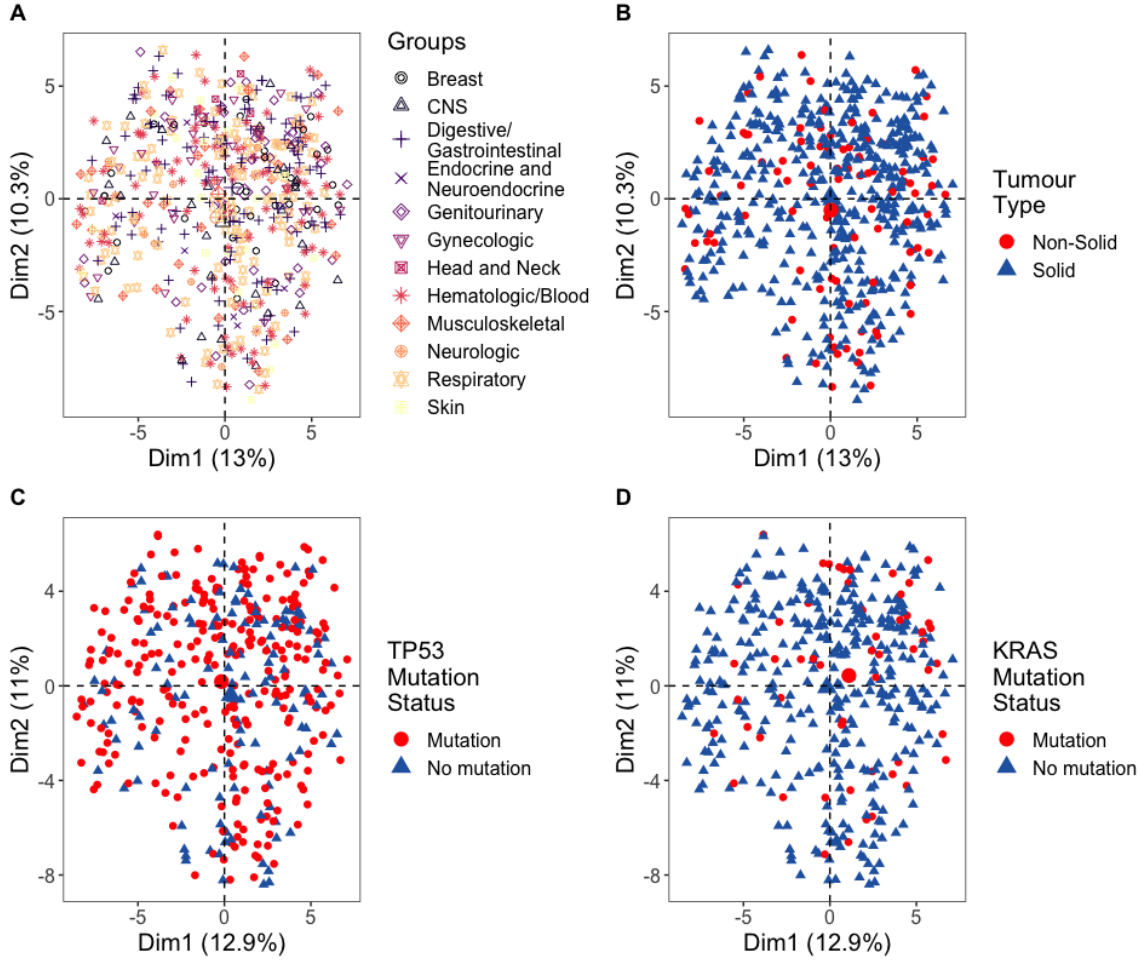
Figure 2: Principal component analysis of pan-cancer cell line therapeutic efficacy, generated from $IC_{50}$ values of all available chemotherapeutics.The horizontal axis shows the first principal component, the vertical axis the second component. Cell lines are visualized based on major cancer type classifications, including (**A**) body system of tumour and (**B**) solid vs. non-solid tumour status. Cell lines were also visualized on major molecular markers, including (**C**) TP53 mutation status, and (**D**) KRAS mutation status.

## 2.4 Classification of cell lines using an optimized neural network

The neural network was constructed using the Tensorflow Keras sequential deep learning API in Python 3. The model underwent multiple instances of optimization, starting with the manipulation of the overall hidden layer architecture. The classifier's predictive accuracy and misclassification rate were monitored to determine the optimal number of dense hidden layers (Fig. 4a) in addition to iterative manipulation of the number of neurons in each hidden layer. The rectified linear unit (ReLu) was chosen as the neuronal activation function for all the layers except for the output layer which used a sigmoid activation as a means of classifying instances into binary classes.

The model was rigorously monitored for overfitting on the training dataset. To minimize overfitting, we employed batch normalization layers followed by dropout layers with a 0.3 dropout rate to improve the generalizability of the model.

The dataset was randomly segregated using the Pareto principle where we reserved 80% of the data for training and the remaining 20% for validation [14]. Model selection was performed by hyperparameter tuning using a grid search followed by 5-fold cross-validation (Table 1). We performed a grid search with 3-fold cross-validation on the training data (80% of the dataset; 432 training samples, 541 overall) to determine the parameters which minimize the binary cross-entropy loss function. GridSearchCV from the scikit-learn library was used as a means of iterating through multiple possibilities of epochs, batch size, optimizer, and kernel initializer to find the optimal model (Table 1). To prevent class imbalance during training, we used the Synthetic Minority Oversampling Technique (SMOTE) from the imblearn package for Python 3. Each model's performance was evaluated by the Area Under Curve (AUC) of the receiver operating characteristic (ROC) curve. Performance evaluation of the final model was performed with the testing set.
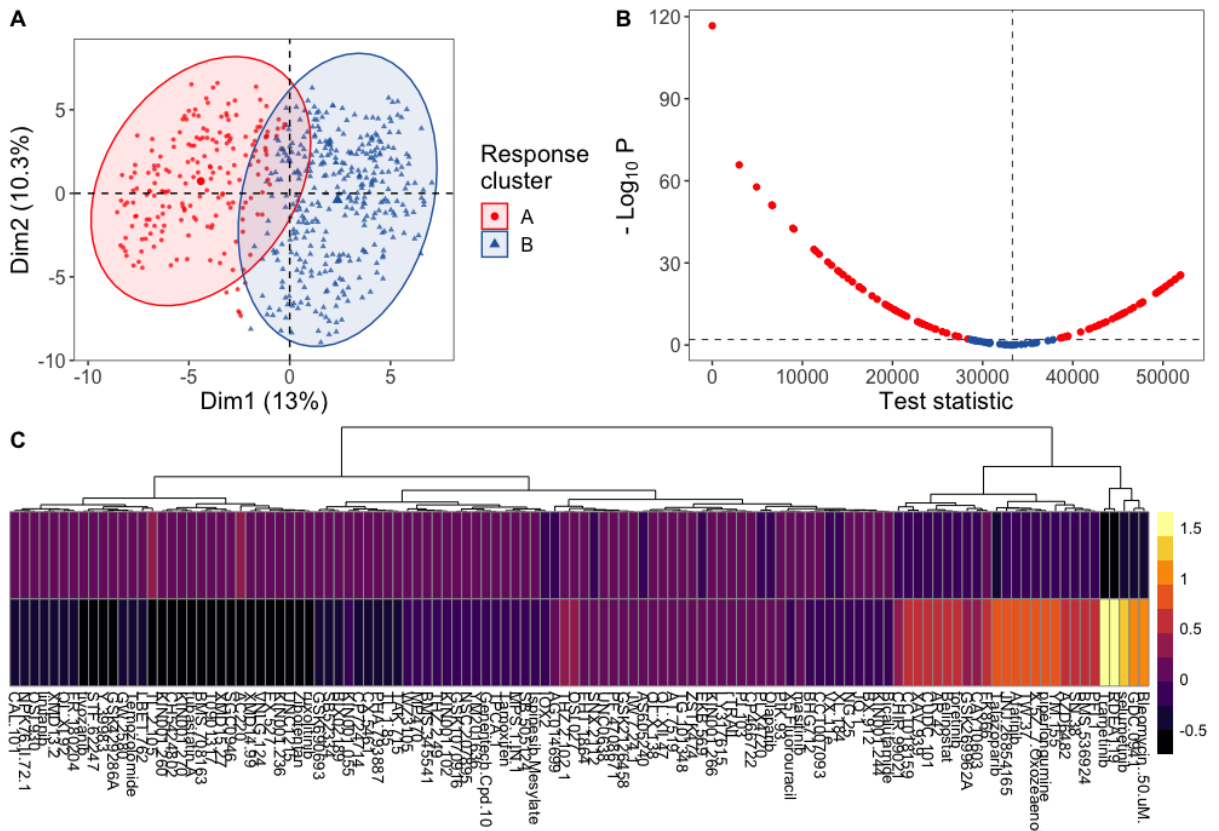
4

Figure 3: (**A**) Principal component analysis of pan-cancer cell line therapeutic efficacy, generated from $IC_{50}$ values of all available chemotherapeutics. The horizontal axis shows the first principal component, the vertical axis the second component. The two identified therapeutic response clusters are indicated in red and blue respectively. (**B**) Volcano plot identifying chemotherapeutics with significantly different $IC_{50}$ values between therapeutic response clusters. Drugs identified in red meet the criteria for significance (FDR adjusted $p < 0.05$). (**C**) Heatmap of therapeutic $IC_{50}$ for the two identified therapeutic response clusters. Columns represent individual chemotherapies and are clustered according to Euclidean distance. Colours range from yellow to black, with a shift toward the latter indicating increased efficacy of the corresponding chemotherapeutic.

## 3 Results

### 3.1 Clustering of pan-cancer cell lines identifies two distinct therapeutic response cohorts

From the GDSC consortium, we included 548 cell lines (49.4% of the original cell lines) and 117 (46.6% of the original drugs) therapeutics for response group clustering. We assessed the ability of common molecular and clinical characteristics to stratify cell lines into groups with similar chemotherapeutic performance by subgrouping cell lines based upon these criteria and plotting them against the first and second principal components. Commonly used measures including the anatomical location and morphologic subtype, as well as TP53 and KRAS mutation status failed to identify defined clusters of cells with similar therapeutic responses (Fig. 2).

To identify defined cohorts of pan-cancer cell lines with similar trends in therapeutic sensitivity, we employed unsupervised clustering of retained cell lines. Principal component analysis was used to reduce the dimensionality of the dataset, allowing for visualization of defined therapeutic response groups. This process identified two distinct clusters of therapeutic sensitivity (Fig. 3), 362 cell lines identified in response group A, and 186 cell lines identified in response group B. The cohorts perform substantially differently in a subset of therapeutics (Fig. 3). To quantify differences in therapeutic response between clusters, IC50 values were compared between candidate cell lines (Fig. 3). Of the 117 therapies included, 95 had significant differences in efficacy between the two cohorts identified. This suggests that these cohorts represent groups of cell lines with vastly different therapeutic responses. Therefore the ability to accurately stratify into these cohorts may be a valuable tool for stratification prior to chemotherapeutic treatment.
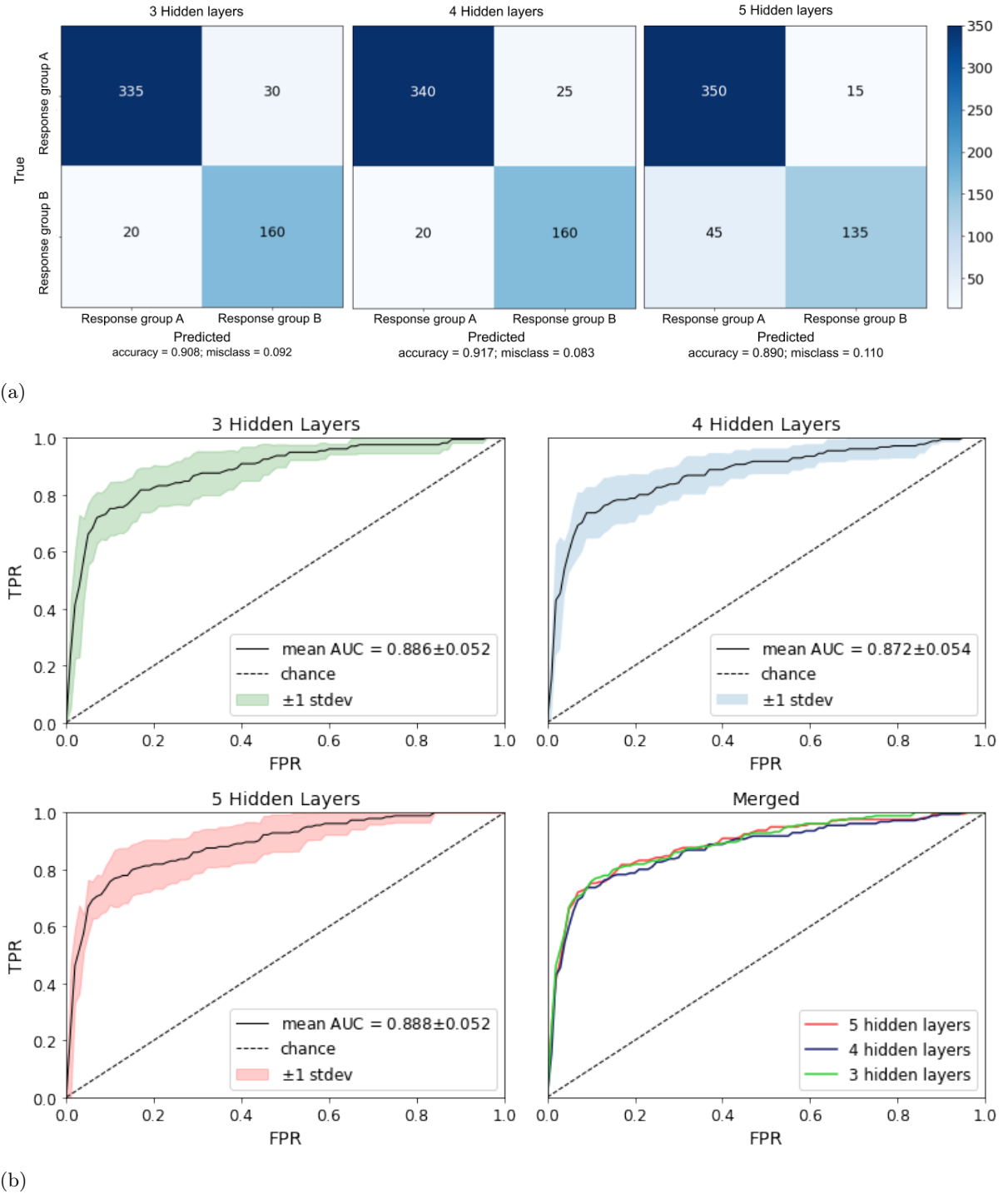
(a)



(b)

Figure 4: (4a) From left to right: confusion matrices for the 3, 4, and 5 hidden layer neural network models evaluating the true positive, false positive, true negative, and false negative rate. The models classify cell line microarray datasets into chemotherapy response cohorts. (4b) ROC curves for 3, 4, and 5 hidden layers neural network models with confidence bands of ±1 standard deviations. Each model was subject to 5-fold cross-validation, and the mean ROC curve across all trials was plotted.

## 3.2 Boruta selects 300 genes from the 16,382 gene dataset

To select genes that are estimated to have the highest predictive value rather than biological significance, the Boruta feature selection algorithm was used. The feature selection algorithm identified 300 relevant genes from the original set of 16,382 genes at $\alpha = 0.05$ with a maximum tree depth of 5. To better understand the transcriptomic heterogeneity underlying the therapeutic response cohorts, a KEGG pathway enrichment analysis was performed on feature-selected genes used in the deep learning model. This analysis identified enrichment of gene sets associated with focal adhesion and PI3K signalling among others (Fig. 5).
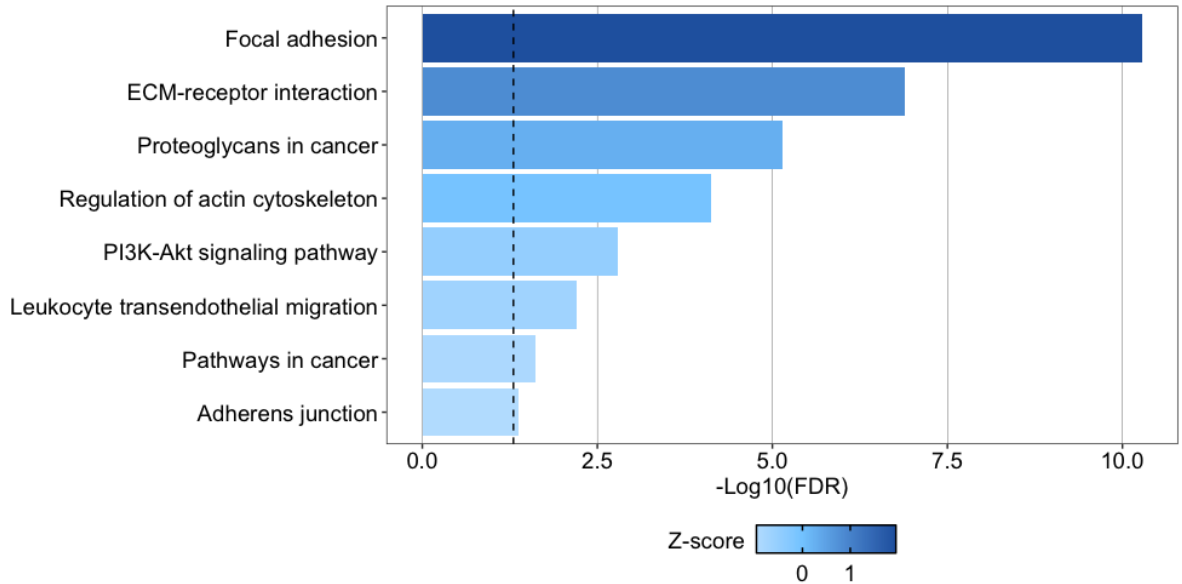
Figure 5: KEGG pathway functional enrichment for feature-selected genes included in the deep learning model. The vertical dotted line indicates the threshold for significance (adjusted $p < 0.05$).

### 3.3 A neural network with four hidden layers accurately classifies patients into responder and non-responder cohorts

Unsupervised learning in the form of the k-means clustering of the cancer cell line transcriptomes indicated substantially different responses to chemotherapies. Using these distinct therapy response cohorts, we developed a deep learning binary classifier to predict drug response groups based on transcriptome data. We initially analyzed five neural network architectures, each corresponding to 1-5 hidden layers (Fig. 6). Hyperparameter optimization via grid search returned similar results for each model: 50 epochs, batch size of 32, Adagrad as the optimizer, and a normal kernel initializer. Neural network architectures containing 3-5 hidden layers performed similarly with approximately 90% accuracy. The architectures with 1 and 2 hidden layers performed less optimally with approximately 80% accuracy. We proceeded to validate the architectures with 3-5 hidden layers using 5-fold cross-validation. Of note, the model with 4 hidden layers had the lowest false positive rate (FPR, 11.11%) and false negative rate (FNR, 6.85%). The model with five hidden layers had the highest FPR (25%) of the models evaluated.

An ROC curve was plotted for each of the neural network variants as an alternative evaluative method under uneven class sizes (Fig. 4b). The relative ratio between the model's FPR and its true positive rate were averaged between 5 k-folds. The mean AUC for the 5 trials was used to compare the three network architectures. However, the differences between the various architectures for AUC was not significantly different. Consequently, confusion matrices (Fig. 4a) and associated misclassification rates were used to pick the optimal model.

The neural net with 4 hidden layers demonstrated the best performance overall with a 91.7% accuracy.

## 4 Discussion

It is well known that there is substantial heterogeneity with respect to chemotherapeutic response between and among cancer types. Although there have been multiple attempts to identify molecular and clinical features predictive of response to particular targeted therapies, there remains considerable variability within subgroups identified using these factors. In this study, we attempt to accurately cluster cancer cell lines into defined groups based on response to a large range of chemotherapeutics, and to create a deep learning transcriptomic model capable of accurately categorizing samples into these defined groups. Using cell line chemotherapeutic efficacy data obtained from the GDSC consortium, we employ unsupervised clustering techniques to identify two defined therapeutic response groups with significantly different responses to a multitude of standard chemotherapies. We show that these clusters outperform classical clinical criteria for classifying samples into chemotherapeutic response groups, and therefore may prove useful for clinical and research settings. To classify cell lines into these groups, we use a biologically agnostic feature selection algorithm, Boruta, to reduce the original set of 16,382 genes to a subset of 300 genes, which was key to limiting preliminary bias in the model. These genes were fed into neural networks, which were then optimized. We determined from confusion matrices and ROC curve analysis that the best network architecture utilized 4 hidden layers, and demonstrated a 91.7% accuracy in classifying response groups. This validates our postu-

late that gene expression is a prime determinant of chemotherapeutic response, and that cell lines of similar gene expression profile respond similarly to most chemotherapies.

The comparatively lower accuracy of the neural networks with 1 and 2 hidden layers (82.6% and 70.8% respectively) suggests that the therapeutic response cohorts cannot be separated by a linear classifier, and further suggests that classical machine learning techniques are insufficient to capture the complexity of the dataset. Furthermore, the high FNR of the network with 5 hidden layers as compared to the 3 and 4 hidden layer networks indicates overfitting. To this end, either a 3 or 4 hidden layer network is the ideal architecture for analyzing our data. Interestingly, there is no significant difference between the mean AUC for these models (Fig. 4b). Given that there were no significant differences between the mean AUC for these models, the FPRs and FNRs were used to select the 4 hidden layer deep learning architecture as our model of choice.

The deep learning transcriptomic model consists of 300 genes, with KEGG pathway enrichment suggesting that predictive genes are associated with numerous pathways, most notably PI3K signalling and focal adhesion. Interestingly, there is a growing body of literature that suggests that PI3K/Akt pathway dysregulation may be associated with chemotherapeutic resistance in numerous different cancer and treatment contexts [15]. Several studies have identified increases in Akt signalling in cancer cell lines exposed to chemotherapy and radiotherapy [16, 17, 18]. Moreover, significant increases in Akt have been identified in chemoresistant and radioresistant cancer models [19]. Similarly, several studies have identified focal adhesion as a potential protective mechanism for various cancer cells. In fact, inhibition of particular integrin isoforms has been shown to increase the susceptibility of various cancer cell lines to conventional chemo/radiotherapies [20]. Our results provide further evidence that dysregulation of PI3K signalling and focal adhesion may play a role in chemotherapy resistance in a pan-cancer context.

A major limitation of our study was the availability of large datasets to train our model. Here we faced a $p \gg n$ problem as machine learning models expect that the number of observations $n$ will be much larger than the number of features $p$. To minimize this bias, we applied the Boruta algorithm to reduce our 16,382 genes by 541 cell lines dataset to a 300 by 541 matrix. The algorithm has been shown in various studies to be an effective feature selection method in high dimensional omics datasets [21]. To prevent overfitting of the reduced matrix, we applied batch normalization and dropout layers immediately preceding each hidden layer. Of note, a neural network architecture where the initial hidden layers diverge and the latter hidden layers converge provides the most accurate classifications of the cell

line microarray data.

Future investigations will look to validate the predictive ability of the model to categorize chemotherapeutic response in various cancer types using the current transcriptomic signature. It is likely that the model accuracy will vary between therapy targets, and as such, further studies can make use of our project pipeline to create a stratified model whereby the drug class and target are additional inputs. Furthermore, it may be interesting to select relevant genes using a different feature selector given that Boruta specifically operates on patterns of statistical relationships rather than biological relationships. Our use of Boruta was motivated by its efficacy demonstrated by prior studies of the algorithm as compared to other feature selectors [21, 22]. It is possible that a feature selection method informed by gene function and linkage disequilibrium could yield a different set of relevant genes.

# 5    Conclusions

Using transcriptomic data from pan-cancer cell lines, two chemotherapeutic response clusters were identified via unsupervised learning in the form of k-means clustering. A feature selection algorithm was used to select a 300 gene subset which served as inputs to multiple neural networks. We determined that the network with 4 hidden layers was the most accurate model, producing a binary classifier to predict cell line therapy response with 91.7% accuracy. Future studies will investigate the efficacy of our model to predict chemotherapy response in various cancer types and treatment contexts.

# Acknowledgements

# References

[1] Akshat Pathak, Sanskriti Tanwar, Vivek Kumar, and Basu Dev Banarjeec. Present and future prospect of small molecule & related targeted therapy against human cancer. *Vivechan Int J Resp*, 9(1):36–49, March 2018.

[2] Brian A Baldo and Nghia H Pham. Adverse reactions to targeted and non-targeted chemotherapeutic drugs with emphasis on hypersensitivity responses and the invasive

metastatic switch. *Cancer Metastasis Rev*, 32(3-4):723–761, December 2013.

[3] Joseph A. Sparano, Robert J. Gray, Della F. Makower, Kathleen I. Pritchard, Kathy S. Albain, Daniel F. Hayes, Charles E. Geyer Jr, Elizabeth C. Dees, Matthew P. Goetz, Jr. John A. Olson, Tracy Lively, Sunil S. Badve, Thomas J. Saphner, Lynne I. Wagner, Timothy J. Whelan, Matthew J. Ellis, Soonmyung Paik, William C. Wood, Peter M. Ravdin, Maccon M. Keane, Henry L. Gomez Moreno, Pavan S. Reddy, Timothy F. Goggins, Ingrid A. Mayer, Adam M. Brufsky, Deborah L. Toppmeyer, Virginia G. Kaklamani, Jeffrey L. Berenberg, Jeffrey Abrams, and George W. Sledge. Adjuvant chemotherapy guided by a 21-gene expression assay in breast cancer. *N Engl J Med*, 379(2):111–121, July 2018.

[4] Kevin Shee, Jason D. Wells, Amanda Jiang, and Todd W. Miller. Integrated pan-cancer gene expression and drug sensitivity analysis reveals slfn11 mrna as a solid tumor biomarker predictive of sensitivity to dna-damaging chemotherapy. *PLoS One*, 14(11):e0224267, November 2019.

[5] Xuewei Wang, Zhifu Sun, Michael T Zimmermann, Andrej Bugrim, and Jean-Pierre Kocher. Predict drug sensitivity of cancer cells with pathway activity inference. *BMC Med Genomics*, 12(15), January 2019.

[6] Wanjuan Yang, Jorge Soares, Patricia Greninger, Elena J Edelman, Howard Lightfoot, Simon Forbes, Nidhi Bindal, Dave Beare, James A Smith, I Richard Thompson, Sridhar Ramaswamy, P Andrew Futreal, Daniel A Haber, Michael R Stratton, Cyril Benes, Ultan McDermott, and Mathew J Garnett. Genomics of drug sensitivity in cancer (gdsc): A resource for therapeutic biomarker discovery in cancer cells. *Nucleic Acids Res*, 41:D955–61, November 2012.

[7] Mehreen Ali and Tero Aittokallio. Machine learning and feature selection for drug response prediction in precision oncology applications. *Biophys Rev*, 11(1):31–39, February 2019.

[8] Stacey Shiovitz and William M Grady. Molecular markers predictive of chemotherapy response in colorectal cancer. *Curr Gastroenterol Rep*, 17(2):431, February 2015.

[9] Vincenzo Catalano, Anna Maria Baldelli, Paolo Giordani, and Stefano Cascinu. Molecular markers predictive of response to chemotherapy in gastrointestinal tumors. *Crit Rev Oncol Hemat*, 38(2):93–104, May 2001.

[10] Ikuo Sekine, John D Minna, Kazuto Nishio, Tomohide Tamura, and Nagahiro Saijo. A literature review of molecular markers predictive of clinical response to cytotoxic chemotherapy in patients with lung cancer. *J Thorac Oncol*, 1(1):31–37, January 2006.

[11] I F Faneyte, J G Schrama, J L Peterse, P L Remijnse, S Rodenhuis, and M J van de Vijver. Breast cancer response to neoadjuvant chemotherapy: predictive markers and relation with outcome. *Br J Cancer*, 86:406–412, February 2003.

[12] Huan Liu. *Feature Selection*, pages 402–406. Springer US, Boston, MA, 2010.

[13] Rudnicki W. Kursa, M. Feature selection with the boruta package. *Journal of Statistical Software*, 36(11), 2010.

[14] Shie-Yui Liong, Soon-Thiam Khu, and Weng-Tat Chan. Derivation of pareto front with genetic algorithm and neural network. *Journal of Hydraulic Engineering*, 6(1), January 1998.

[15] Wei-Chien Huang and Mien-Chie Hung. Induction of akt activity by chemotherapy confers acquired resistance. *Journal of the Formosan Medical Association*, 108(3):180 – 194, 2009.

[16] J M Nelson and D W Fry. Akt, mapk (erk1/2), and p38 act in concert to promote apoptosis in response to erbb receptor family inhibition. *J Biol Chem*, 276:14842–14847, 2001.

[17] S S Ng, M S Tsao, and T Nicklee. Wortmannin inhibits pkb/akt phosphorylation and promotes gemcitabine anti-tumor activity in orthotopic human pancreatic cancer xenografts in immunodeficient mice. *Clin Cancer Res*, 7:3269–3275, 2001.

[18] S S W Ng, M S Tsao, and S Chow. Inhibition of phos-phatidylinositide 3-kinase enhances gemcitabine-induced apoptosis in human pancreatic cancer cells. *Cancer Res*, 60:5451–5455, 2000.

[19] K. Yokoi, A. Kobayashi, H. Motoyama, M. Kitazawa, A. Shimizu, T. Notake, T. Yokoyama, T. Matsumura, M. Takeoka, and S. I. Miyagawa. Survival pathway of cholangiocarcinoma via akt/mtor signaling to escape raf/mek/erk pathway inhibition by sorafenib. *Oncology reports*, 39(2):843–850, Feb 2018. LR: 20181202; JID: 9422756; 0 (FOXO1 protein, human); 0 (Forkhead Box Protein O1); 0 (Phenylurea Compounds); 0 (Protein Kinase Inhibitors); 25X51I8RD4 (Niacinamide); 9HW64Q8G6G (Everolimus); 9ZOQ3TZI87 (Sorafenib); EC 2.7.1.1 (MTOR protein, human); EC 2.7.1.1 (TOR Serine-Threonine Kinases); EC 2.7.11.1 (Proto-Oncogene Proteins c-akt); 2017/07/12

00:00 [received]; 2017/12/07 00:00 [accepted]; 2017/12/19 06:00 [entrez]; 2017/12/19 06:00 [pubmed]; 2018/08/24 06:00 [medline]; ppublish.

[20] Iris Eke and Nils Cordes. Focal adhesion signaling and therapy resistance in cancer. *Seminars in Cancer Biology*, 31:65 – 75, 2015. Intracellular Signaling and Response to Anti-Cancer Therapy.

[21] Frauke Degenhardt, Stephan Seifert, and Silke Szymczak. Evaluation of variable selection methods for random forests and omics data sets. *Brief Bioinform*, 20(2):492–503, March 2019.

[22] Theodore Sakellaropoulos, Konstantinos Vougas, Sonali Narang, Filippos Koinis, Athanassios Kotsinas, AlexanderPolyzos, Tyler J Moss, Sarina Piha-Paul, Hua Zhou, Eleni Kardala, Eleni Damianidou, Leonidas G Alexopoulos, Iannis Aifantis, Paul A Townsend, Mihalis I Panayiotidis, Petros Sfikakis, Jiri Bartek, Rebecca C Fitzgerald, Dimitris Thanos, Kenna R Mills Shaw, Russell Petty, Aristotelis Tsirigos, and Vassilis G Gorgoulis. A deep learning framework for predicting response to therapy in cancer. *Cell Reports*, 29(11):3367–3373, December 2019.
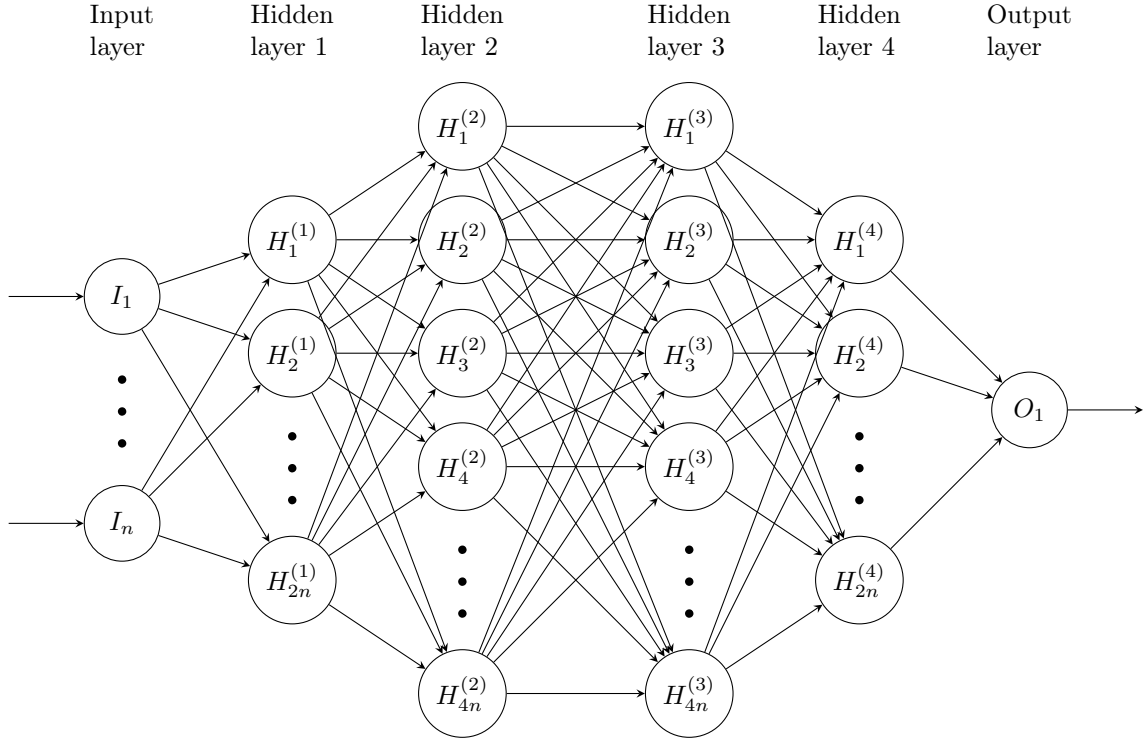
# Supplementary Data

**Figures**



Figure 6: Neural network architecture representation with four hidden layers ($n = 300$). Inputs include the feature-selected genes from the cell line microarray dataset. Each hidden layer has a dropout rate of 0.3 and is subject to batch normalization.

**Tables**

Table 1: Grid search parameters to optimize all implemented neural network architectures (3, 4, and 5 hidden layers). Each grid search underwent 3-fold cross-validation on the training data.

| Epochs | Batches | Optimizer | Kernel initializer |
|--------|---------|-----------|--------------------|
| 25 | 16 | Stochastic gradient descent | Normal |
| 50 | 32 | Adagrad | Uniform |
| 75 | 64 | Adam | Glorot uniform |

Table 2: Neural network architectures and the number of neurons per layer ($n = 560$).

| Architecture | Number of neurons |
|--------------|-------------------|
| 5 hidden layers | 300 inputs, $2n$, $4n$, $4n$, $2n$, $n$, binary output |
| 4 hidden layers | 300 inputs, $2n$, $4n$, $4n$, $2n$, binary output |
| 3 hidden layers | 300 inputs, $2n$, $4n$, $2n$, binary output |